TM-1173
8055.000

120 GeV PROTON TRANSPORT FOR ANTIPROTON PRODUCTION IN THE FERMILAB TEVATRON I PROJECT*

E. Colton+, C. Hojvat, and L. Oleksiuk

March 1983

* Presented at the 1983 Particle Accelerator Conference, Santa Fe New Mexico, March 21-24.
+ Argonne National Laboratory

120 GEV PROTON TRANSPORT FOR ANTIPROTON PRODUCTION IN THE FERMILAB TEVATRON I PROJECT

Eugene Colton
Argonne National Laboratory+
and
Carlos Hojvat and Les Oleksiuk
Fermi National Accelerator Laboratory*
Batavia, Ill. U.S.A. 60510.

Summary

Short bunches of 120 GeV protons will be used for the production of 8 GeV antiprotons. Protons will be extracted vertically from the Main Ring using two high field Lambertson type magnets at location F17. The beam transport is made of three sections: horizontal dispersion cancellation, vertical dispersion cancellation and final focusing. The final focusing section is composed of two quadrupole doublets and allows for variation in β^* values at the target from 1.5 m to 20.0 m.

Introduction

The Fermilab Tevatron I project will enable Fermilab to produce proton-antiproton collisions in the Tevatron accelerator.[1] Production of antiprotons for cooling and accumulation utilizes 120 GeV protons from the Main Ring accelerator. The choice of the parameters to optimize the production and collection of antiprotons is discussed elsewhere.[1,2]

The time structure of the proton beam is transfered to the antiprotons produced at the target. The longitudinal emittance of the antiprotons (for a given $\Delta p/p$) can be minimized by preparing the protons into short bunches, before extraction and targeting. Equally, the transverse emittance of the antiprotons (for a given collection angle) can be minimized by reducing the proton beam spot at the target, down to sizes that are compatible with operating the target without immediate destruction.

After cooling and accumulation the antiprotons are to be transported back, bypassing the target, through the proton transport line for injection into the Main Ring. The design of the proton line must satisfy the following requirements: i) Geometrical constraints for the location of the target station. ii) Leave the Main Ring tunnel as close as possible to the extraction point. iii) Transport a 120 GeV beam of transverse emittance $0.2\pi \times 10^{-6}$m in both planes and $\Delta p/p = \pm 0.2\%$. iv) Transport back the 8.0 GeV cooled antiprotons beam with an emittance of $2.0 \times 10^{-6}\pi$m in both planes. v) Zero dispersion at the target with a round spot of variable size from 0.2mm to 0.8mm rms.

The location of the proton transport line with reference to the other accelerators and the antiproton source at Fermilab is shown in Figure 1.

Transport Line

A. Transport Section

The first part of the beam line separates the proton beam away and up from the Main Ring, to follow a convenient path so as to be aimed at the target location. Following the two Lambertson extraction septa the rising beam is bent left and down by four EPB (External Proton Beam) 10 foot dipoles. After drifting through a beam pipe (26 m separating the Main Ring tunnel from the beam transport enclosure, the beam is bent right and down. Three of the dipoles were rotated by 45° in order to accomplish the combined operation along with five dipoles placed conventionally. A further vertical drift is finally terminated by the EPB dipoles which render the beam flat at a height of seven feet above Main Ring elevation. These sections utilize EPB quadrupoles to contain the beam as well as to effect a first-order achromatic transformation. A list of the beam elements is provided in Table I, the maximum quadrupole strength achievable is 19T/m.

B. Lambertson Magnets

In order to reach 120 GeV extraction from the Main Ring, within the geometrical conditions imposed, two high field Lambertson magnets with the characteristics listed in Table II are required.

A single lamination design will be used for both upstream and downstream modules. The resulting magnet geometry is shown in Figure 2. The large horizontal proton beam size arising from the dispersion at F17 (5.647 m) sets the requirement of a field gap of 1.65". Extensive modelling[3] was performed on the lamination design to ensure that optimum magnetic flux balancing occurred near the field free channel containing the Main Ring beam. Both yoke asymmetry and pole chamfering were utilized to minimize the leakage field. Allowed gradients were kept below the half integer stop band width ($\Delta\nu = 0.02$) at 120 GeV/c. Ramped operation of the magnets is required so as not to perturb the low energy circulating beams. Leakage fields at the magnet ends will typically add 50% to the fields appearing in the field free channel - the end effects were also modelled for the design of a mirror plate shunt configuration to reduce this contribution to the order of 15%. The good field region of this design spans a width of 7.0" with a required uniformity of 0.2%, based on the expected beam vertical divergence. The computer predicted field uniformity is shown in Figure 3 for an excitation value of 1.28 T. The uniformity is given as the field deviation 0.5" from the median plane, corresponding to the expected horizontal beam radius.

C. Final Focusing Section

The beam arriving at the start of the final focusing section (PQ6A) is dispersion free ($\eta_x = \eta'_x = \eta_y = \eta'_y = 0$) and is described by the Twiss parameters $\beta_x = 22.78125$m, $\alpha_x = -1.2588$, $\beta_y = 117.9955$m and $\alpha_y = -6.68625$. These conditions are transformed to the desired conditions at the antiproton ($\bar{p}$) production target; they also represent the match conditions for the returning flux of 8 GeV cooled antiprotons. The final beam size is achieved by two quadrupole doublets, with each component being two EPB 3Q120 quadrupoles running with the same

† Now at Los Alamos National Laboratory
+ Operated for the U.S. Department of Energy by the University of Chicago
* Operated by the Universities Research Association, Inc., under contract with the U.S. Department of Energy.

strength. A wide tuning range allows the formation of round target spots ($\beta_x = \beta_y$) with $1 < \beta < 19$m. To illustrate the coverage of the final tuning range we show in Table III the gradients of the final quadrupoles for the listed target waists $\beta^* = \beta_x = \beta_y$ ($\alpha_x = \alpha_y$). The factor of x16 range in beta results in a factor of x4 variation in size, 0.2mm $< \sigma < 0.8$mm for a proton beam emittance of 0.2π mm-mr.

In Fig. 4 we show the distribution of monoenergetic β and η functions through the system for the magnets as in Table I.

Reverse Transport of Cooled $\bar{p}$

The beam must transport back an 8 GeV $\bar{p}$ beam with a transverse emittance of $\epsilon_T = 2.0\pi$ mm-mr with very small $\delta p/p < 10^{-4}$. Therefore the envelope functions have been limited to $\beta_y < 330$ m and $\beta_x < 550$ m. The tunes are identical to the 120 GeV proton values starting at the match point (upstream end of PQ6A) and proceeding upstream to the Main Ring. Between quadrupoles PQ7B and PQ8A is located a 4.5° bending magnet; the cooled $\bar{p}$ bypass the target and return through this bending magnet to the 120 GeV transport line.

Chromatic Aberrations

The only aberrations which might contribute to increased proton spot size at the $\bar{p}$ production target are the chromatic terms. We have calculated the aberrations for the worst possible case ($\beta^* = 1.17$m). The terms are presented in Table IV along with the maximum contributions to the spot size expected. The terms are small. Presumably dipole errors will create worse aberrations and sextupole correction may be required.

References

1. Design Report Tevatron I Project, October 1982, Fermilab.

2. "Calculation of Antiproton Yields for the Fermilab Antiproton Source," C. Hojvat and A. Van Ginneken, Fermilab-PUB-82/43. (Nuc. Inst. Meth. to be published)

3. "Design of a High Field Lambertson Magnet for the F-17 Extracted Beam", L. Oleksiuk, Fermilab $\bar{p}$ note #249, November 1982.

Figure Captions

Figure 1: Location of the proton transport line and the Antiproton source.

Figure 2: proposed lamination for the F17 extraction Lambertson magnets

Figure 3: Calculated field uniformity of the proposed Lambertson magnets 0.5" from the median plane.

Figure 4: Monoenergetic β and η functions for the 120 GeV proton line.

TABLE I Transport Elements

NAME	DIST. TO F17(m)	TYPE	FIELD/GRADIENT (T) or (T/m)	FUNCTION
P-LAM1	2.74	Lamb.	1.28	Bend up
P-LAM2	8.38	Lamb.	1.28	Bend up
PB1	21.7	EPB	1.271	Bend Left
PB2	25.0	EPB	1.271	Bend Left
PBR1	28.4	EPB(R)	1.271	Bend Left/Down
PBR2	31.7	EPB(R)	1.271	Bend Left/Down
PQ1	35.1	3Q120	6.59	Vert. Focusing
PQ2	64.2	3Q120	4.85	Vert. Focusing
PBR3	67.5	EPB(R)	1.271	Bend Right/Down
PB3	70.9	EPB	1.271	Bend Right
PB4	74.2	EPB	1.271	Bend Right
PB5	77.6	EPB	1.271	Bend Right
PQ3	80.9	3Q120	12.09	Horiz. Focusing
PQ4	94.1	3Q120	15.96	Vert. Focusing
PQ5A	107.3	3Q120	18.30	Horiz. Focusing
PQ5B	110.7	3Q120	18.30	Horiz. Focusing
PBV1	123.7	EPB	0.782	Bend Down
PBV2	127.0	EPB	0.782	Bend Down
PQ6A	130.7	3Q120	11.43	Vert. Focusing
PQ6B	134.1	3Q120	11.43	Vert. Focusing
PQ7A	139.6	3Q120	10.27	Horiz. Focusing
PQ7B	143.0	3Q120	10.27	Horiz. Focusing
PQ8A	154.9	3Q120	12.38	Vert. Focusing
PQ8B	158.3	3Q120	12.38	Vert. Focusing
PQ9A	163.9	3Q120	9.27	Horiz. Focusing
PQ9B	167.2	3Q120	9.27	Horiz. Focusing
TARGET	174.1			

TABLE II
Characteristics of F-17 Lambertson Magnets

Magnet length	204" (x 2 units)
Gap field (for 120 GeV/c)	1.28 T
Vertical beam excursion	7.0" total
Bend angle	33.0 mrad total
Field gap	1.65"
Field Free Channel Maximum gradient	0.08 T/m (for 408")
Number of turns	40
Power	49 KW DC @ 1300 A
Current density	424 A/cm² @ 1.32 T
Inductance (low field)	80 mh

TABLE III
Gradient of Final Focusing Quadrupoles as a Function of Beam Size at the Target, in T/m

β^*(m)	σ(mm)	PQ6A/B	PQ7A/B	PQ8A/B	PQ9A/B
1.17	0.20	-13.2	+10.3	-12.1	+13.2
4.69	0.40	-11.4	+10.3	-12.4	+ 9.3
18.75	0.79	-10.3	+ 9.7	- 9.8	+ 2.0

TABLE IV Chromatic Abberrations Terms

Term	Value		Max Aberration
$(x\|x_0\delta)$	3.917×10^{-2}	mm/mm(%)	0.0270 mm
$(x\|x_0'\delta)$	-0.226	mm/mr(%)	0.0034 mm
$(x\|\delta^2)$	-2.03×10^{-2}	mm/(%)^2	0.0008 mm
$(y\|y_0\delta)$	-0.271	mm/mm(%)	0.1030 mm
$(y\|y_0'\delta)$	2.238	mm/mr(%)	0.0330 mm
$(y\|\delta^2)$	0.175	mm/(%)^2	0.0070 mm

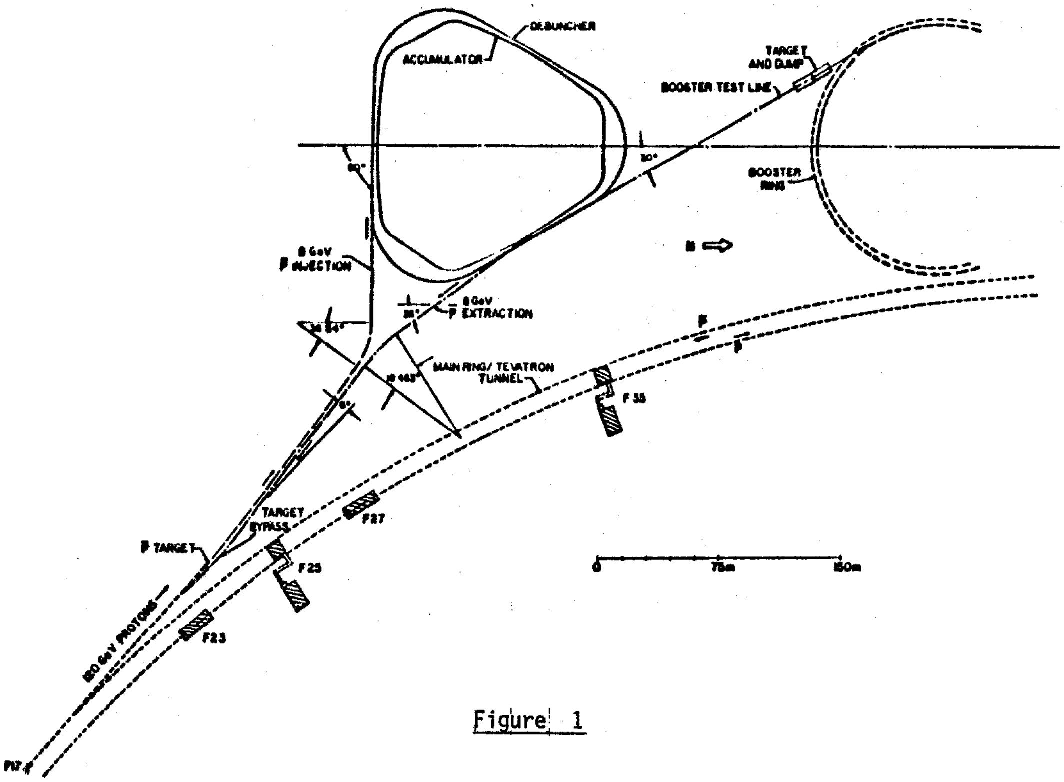

Figure 1

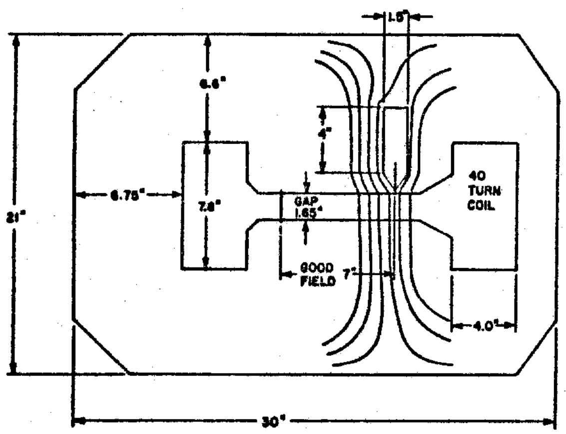

Figure 2

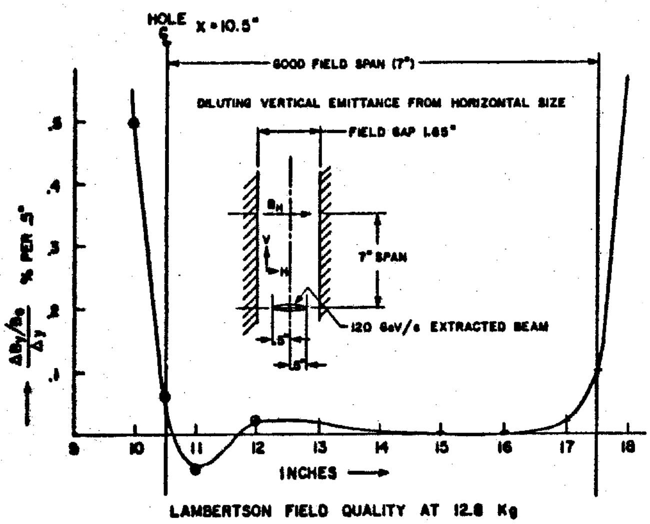

Figure 3

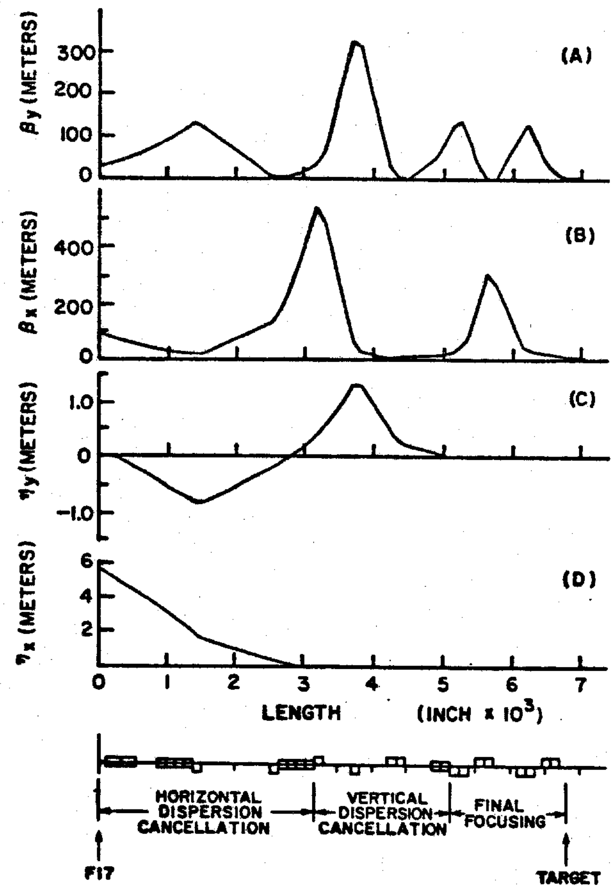

Figure 4